Investigation of Chemical Stabilities and Contact Angle of 3D Printed Polymers with CO₂ Capture Solvents to Enhance Absorber Performance

Moushumi Sarma[a], Keemia Abad[a,b], Du Nguyen[c], Samantha Ruelas[c], Kunlei Liu[a,d,*],

Jesse Thompson[a,b,*]

[a]Univeristy of Kentucky, Center for Applied Energy Research, Lexington, KY, 40511, USA,

[b]University of Kentucky, Department of Chemistry, Lexington, KY, 40506, USA

[c]Lawrence Livermore National Laboratory, Livermore, CA, 94550, USA

[d]University of Kentucky, Department of Mechanical Engineering, Lexington, KY, 40506, USA

*To whom correspondence should be addressed to E-mail: jesse.thompson@uky.edu and Phone:

+1 (859)-257-0355, E-mail: kunlei.liu@uky.edu and Phone: +1 (859)-257-0293,

Abstract

Increasing absorption rate in aqueous amine CCS systems is one avenue to decrease capital cost by reducing the overall size of the absorber column. One potential route is by replacing conventional steel packing with custom designed packing made from 3D printed polymers. 3D printing offers endless flexibility in packing designs to better enhance liquid/gas contact, increase CO_2 mass transfer and create compact absorber columns. Before exploring novel packing designs, it is necessary to identify polymer materials that can be 3D printed while also showing long-term physical and surface property stability upon exposure to corrosive amine solutions. Four polymers that are commonly used for 3D printing were evaluated using CO_2-loaded amine solution at temperatures typically observed in the absorber column. Three polymers, high-density polystyrene (HDPS), acrylonitrile butadiene styrene (ABS) and nylon were found to be physically stable after 5000 hr of amine exposure at temperatures up to 60 °C. The contact angle (wetting) of water and CO_2-loaded aqueous amine solution on the polymer surfaces were also stable after exposure to the CO_2-loaded amine solution.

Introduction

The emission of greenhouse gas, CO_2 from fossil fuel combustion contributes to an adverse impact on the environment and thus has been the subject of widespread attention over the past few decades. The rise in CO_2 has resulted in increased global warming and climate change (Masson-Delmotte, 2018). Carbon Capture and Storage (CCS) is a process in which CO_2 gas is captured, transported to a suitable storage site and deposited under the ground from which the CO_2 gas cannot come up to the atmosphere (Bui et al., 2018). This concern over the increasing level of CO_2 leads to new regulations on fossil-fuel fired power generation such as Kyoto Protocol (Breidenich et al., 1998; Rogelj et al., 2016). The use of aqueous amine based post-combustion CO_2 capture is the most utilized technique adapted industrially due to its fast kinetics, availability, and relative costs at the required scale (Boot-Handford et al., 2014; Rochelle, 2009; Wang et al., 2011; Yang et al., 2008). In fossil fuel fired power plants, CO_2 can be captured either before (pre-combustion carbon capture) or after fuel combustion (post-combustion carbon capture).

The deployment of post-combustion CO_2 capture can be continued through the development of new technologies and strategies to overcome the remaining challenges related to both operating and capital costs. Increasing absorber efficiency, in aqueous amine CCS systems is one avenue to decrease capital cost by reducing the overall size of the absorber column (Lippert et al., 2014). The recent research toward increasing CO_2 absorption in amine-based CCS processes has focused on three main strategies: (1) solvent development/amine blends (Li et al., 2013; Lin and Wong, 2014; Shi et al., 2014; Voice et al., 2013) (2) the addition of catalysts, such as small-molecule carbonic anhydrase (CA) mimics (Floyd et al., 2013; Koziol et al., 2012; Lippert et al., 2014; Widger et al., 2017; Widger et al., 2019) and (3) modification of the packing

62   material to increase wetted surface area (Tsai et al., 2008; Tsai et al., 2011) to increase the

63   chemical kinetics of absorption and desorption reactions.

64   Absorber column height in a CCS process is directly related to the kinetics of CO_2

65   absorption, thus there has been significant effort toward increasing the mass transfer (K_G) of CO_2

66   in the absorber. Mass transfer enhancement is especially useful at the middle and bottom of the

67   absorber where liquid side mass transfer is limited, and reaction kinetics begin to slow. In

68   addition, increased K_G allows decreased liquid flow, and reduction of the sensible heat

69   requirement for solvent regeneration (Liu et al., 2019). One potential route to improve the

70   absorber performance is by replacing conventional steel packing with custom designed packing

71   made from 3D printed polymers. Steel packing material can corrode upon exposure to the amine

72   solvents. Leclaire and Heldebrant reported replacing stainless steel in the absorber with plastic

73   packing to reduce solvent degradation, which is common in amine systems (Leclaire and

74   Heldebrant, 2018). Other examples of testing of different plastic packings in laboratory-scale

75   continuous flow systems have been reported (Zheng et al., 2020).

76   3D printing (additive manufacturing) methods offer flexibility in reactor/absorber designs

77   to enhance liquid/gas contact and increase absorber column efficiency (Stlaroff, 2017). When

78   considering the use of polymeric 3D printed packing within the absorber column, it will be

79   important to understand how amine solvents will flow down, or wet, these packing surfaces.

80   Wettability studies usually involve the measurement of contact angles as the primary data, which

81   indicates the degree of wetting when a solid and liquid interact. Small contact angles (<< 90°)

82   correspond to high wettability, while large contact angles (>>90°) correspond to low wettability

83   (Law, 2014; Yuan and Lee, 2013). Before exploring novel packing designs, it is necessary to

84   identify polymer materials that can be 3D printed while also showing long-term physical and

85 surface property stability upon exposure to corrosive amine solutions. In this study, four

86 polymers, commonly used in 3D printing are examined for physical and surface stability during

87 long-term exposure to a corrosive CO_2-loaded amine solution at temperatures typically observed

88 in the absorber column. The polymers are high-density polystyrene (HDPS), Acrylonitrile

89 butadiene styrene (ABS), Nylon, and Polylactic acid (PLA). There are a limited number of

90 studies available to understand the wettability of these polymers via contact angle measurements

91 with aqueous amine solutions (Inagaki and Kimura, 2009; Rodríguez-Vidal et al., 2018).

92   This report describes a study of the static contact angles of carbon loaded amine

93 solutions on the different polymer surface. The thicknesses, diameters, weights and stabilities of

94 these polymers were examined after 5000 hrs of exposure of carbon loaded amine solution

95 (C/N~0.4) at 60 °C to replicate typically absorber temperature and loading conditions observed

96 at bench and pilot systems (Frimpong et al., 2019). The static contact angle (wetting) of the

97 polymer surfaces were also examined after exposure to the CO_2-loaded amine solution.

2. Methods

2.1. 3D Printed polymer coupons

100 Polymer coupons were prepared from high-density polystyrene (HDPS), acrylonitrile butadiene

101 styrene (ABS), nylon, and polylactic acid (PLA). The HDPS and ABS were purchased from

102 Keene Village Plastics. The Nylon and PLA were purchased from MatterHackers and Polymaker

103 PolyLite respectively. Sample coupons with a 20 mm diameter and 2 mm thickness were

104 designed using Blender. The generated files were sliced and translated into toolpath code using

105 Cura. A LulzBot Mini 3D printer was used to print HIPS (Keene Village Plastics), ABS (Keene

106 Village Plastics), nylon (MatterHackers), and PLA (Polymaker PlolyLite) coupons—all

107   filaments had a diameter of 2.85 mm. The 3D printer was configured with a 0.4 mm diameter

108   nozzle, a layer height of 0.38 mm was set, and a printing speed of 60 mm/s was used. To print

109   HDPS coupons, a nozzle temperature of 240 °C and bed temperature of 110 °C were used. The

110   ABS coupons required a nozzle temperature of 275 °C and bed temperature of 110 °C. Nylon

111   was printed at 250 °C, with a bed temperature of 75 °C. Finally, a nozzle temperature of 205 °C

112   and bed temperature of 60 °C were used for PLA.

113   **2.2. Polymer stability with amine exposure**

114   The weight, thickness and diameter of each coupon were measured prior to the amine exposure.

115   The static contact angle of water and a CO_2-rich ~5 M 1-Amino-2-Propanol amine solution (C/N

116   ~0.4) on the polymer coupon surface was also measured prior to exposure to the amine solution.

117   The polymer coupons were then placed in a 100 mL-glass bottle and immersed in the 30 mL

118   CO_2-loaded amine solution at room temperature. After 1000 hr the coupons were removed, and

119   all the measurements were repeated. The coupons were then returned to the CO_2-loaded amine

120   solution at 60 °C (in a water bath). The coupons were removed from the solution every 1000 hr

121   and the weight, diameter, thickness, and contact angle measurements were repeated. For the

122   thickness and the diameter measurements, a vernier caliper scale (Mitutoyo Model # 505-736)

123   was used.

124   **2.3. Contact angle measurements**.

125   A Biolin Scientific Optical Tensiometer with One attension software was used to measure the

126   static contact angles. The polymer coupons were polished to use as the surface for contact angle

127   (θ) measurements (**Figure 1**). Each measurement was performed after external calibration of the

128   instrument with a standard calibration ball followed by DI water calibration. The contact angle

129 was measured by the sessile drop method. The contact angle reported in this report are the

130 contact angle measured after 60 seconds of liquid-surface contact. All Contact angles were

131 measured in quadruplicate at 22 °C and the average value is reported.
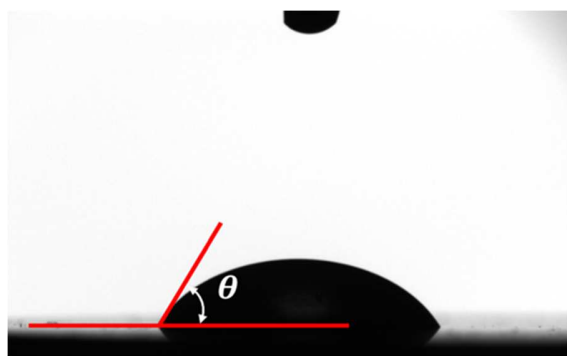
132

133 **Figure 1**. Contact angle (θ) of a CO_2-loaded amine solution on a 3D-printed polymer surface.

134 **2.4. Amine solution preparation**

135 The amines used in this study including Monoethanolamine, 2-Amino-1-Propanol, N-

136 Methylethanolamine, 2-(Ethylamino)ethanol, Dimethylethanolamine, Diethanolamine and N-

137 Methyldiethanolamine were purchased from Sigma Aldrich. Aqueous amine solutions were

138 prepared at ~ 5 M (mol/kg) with deionized water (water content between 50-75%).

139 gravimetrically and loaded with CO_2 using a previously described process (Matin et al., 2016).

140 **3. Results and Discussion**

141 **3.1. Polymer Stability**

142 The durability of several polymers that are commonly used in 3D printing were assessed after

143 exposure to the amine solvent with CO_2-loading (C/N ~0.4) followed as discussed in the

144 experimental section. This process was repeated four additional times, for a total amine solution

145   exposure of 1000 hr at room temperature plus 5000 hr at 60 °C. The HDPS, also commonly

146   called high impact polystyrene (HIPS), ABS and Nylon polymers were essentially unchanged in

147   terms of mass and size at the end of the 6000 hr (1000 hr at room temperature + 5000 hr at 60

148   °C) total exposure time. **Table 1** shows the coupon weight, thickness, diameter, and physical

149   appearance after every 1000 hr. All the measurements were recorded in the quintet and the

150   average value is reported. For HDPS and ABS, the changes in the thickness, diameter, and

151   weights after 6000 hr of amine exposure fall within ±2%. The temperature stability of these

152   materials is very important for the packing material inside the absorber column as any swelling

153   or deformation of the packing can be detrimental. For nylon, the percentage of increase in weight

154   was found to be slightly higher (around ~7%) after 6000 hr of amine exposure. However, the

155   thickness and the diameter remain unchanged before and after amine exposure. The PLA coupon

156   began to decompose during the amine exposure at the elevated temperature. After 1000 hr at 60

157   °C, the PLA coupon deformed (**Figure 2**) and lost its colorings pigment to the amine solution.

158   Eventually, the PLA coupon completely dissolved by the end of 2000 hr at 60 °C.

159

Figure 2. (Top) 3D printed polymer coupons of HDPS, ABS, Nylon, and PLA; (Bottom) Polymer coupons after exposure to CO_2-loaded amine solution for 1000 h at room temperature (± 22 °C) followed by 5000 h exposure at 60 °C (PLA coupon exposure is after 1000 h at 60 °C).

Table 1: Physical appearance of the coupons after amine exposure

Coupon Material	Amine Exposure	Physical Appearance	Weight (in g)	Thickness (in inches)	Diameter (in inches)
HDPS	Before	White	0.655	0.088	0.794
	After 1000 hr at RT	No change	0.655	0.091	0.799
	After 1000 hr at 60 ºC	No change	0.655	0.089	0.795
	After 2000 hr at 60 ºC	No change	0.655	0.089	0.794

	After 3000 hr at 60 ºC	No change	0.657	0.088	0.794
	After 4000 hr at 60 ºC	No change	0.657	0.091	0.795
	After 5000 hr at 60 ºC	No change	0.658	0.089	0.791
% Change		No change	+0.42%	+1.13%	±0.38%
ABS	Before	White	0.566	0.081	0.792
	After 1000 hr at RT	No change	0.566	0.080	0.803
	After 1000 hr at 60 ºC	No change	0.569	0.081	0.799
	After 2000 hr at 60 ºC	No change	0.604	0.081	0.801
	After 3000 hr at 60 ºC	No change	0.571	0.080	0.861
	After 4000 hr at 60 ºC	No change	0.574	0.081	0.800
	After 5000 hr at 60 ºC	No change	0.576	0.081	0.800
% Change		No change	+1.78%	No Change	+1.01%
Nylon	Before	Black	0.571	0.074	0.810
	After 1000 hr at RT	No change	0.585	0.076	0.814
	After 1000 hr at 60 ºC	No change	0.597	0.073	0.812
	After 2000 hr at 60 ºC	No change	0.570	0.074	0.814
	After 3000 hr at 60 ºC	No change	0.591	0.071	0.810
	After 4000 hr at 60 ºC	No change	0.609	0.074	0.820
	After 5000 hr at 60 ºC	No change	0.612	0.075	0.818
% Change		No change	+7.18%	+1.35%	+0.98%
PLA	Before	Bright orange	0.716	0.081	0.807
	After 1000 hr at RT	Discoloration	0.715	0.080	0.831

		occurred			
	After 1000 hr at 60C	Coupon deformed	0.044	NA	NA

164

3.2. Polymer contact angle (wettability)

166 Based on the amine stability observed, the polymeric materials ABS, Nylon and HDPS were

167 identified as stable upon exposure to CO_2-loaded amine solvent at anticipated absorber

168 temperatures (up to 60 °C). The next step was to measure the relative contact angle of these

169 materials and see if the surface properties were impacted by exposure to the amine solution. To

170 assess this, the contact angle of water and the amine solution relative to these polymeric coupon

171 surfaces was also measured after each amine exposure period (**Figure 3**). The contact angle of

172 water and the CO_2-loaded amine solution was also measured before any testing for comparison.

173 The contact angle study, with PLA was performed only before and after 1000 hr of exposure

174 with CO_2-loaded amine exposure at RT due to its instability in amine solution at 60 °C (See

175 Supporting Information). A table of the static contact angles with water and CO_2-loaded amine

176 on the different polymer surfaces before and after amine exposure are reported in the Supporting
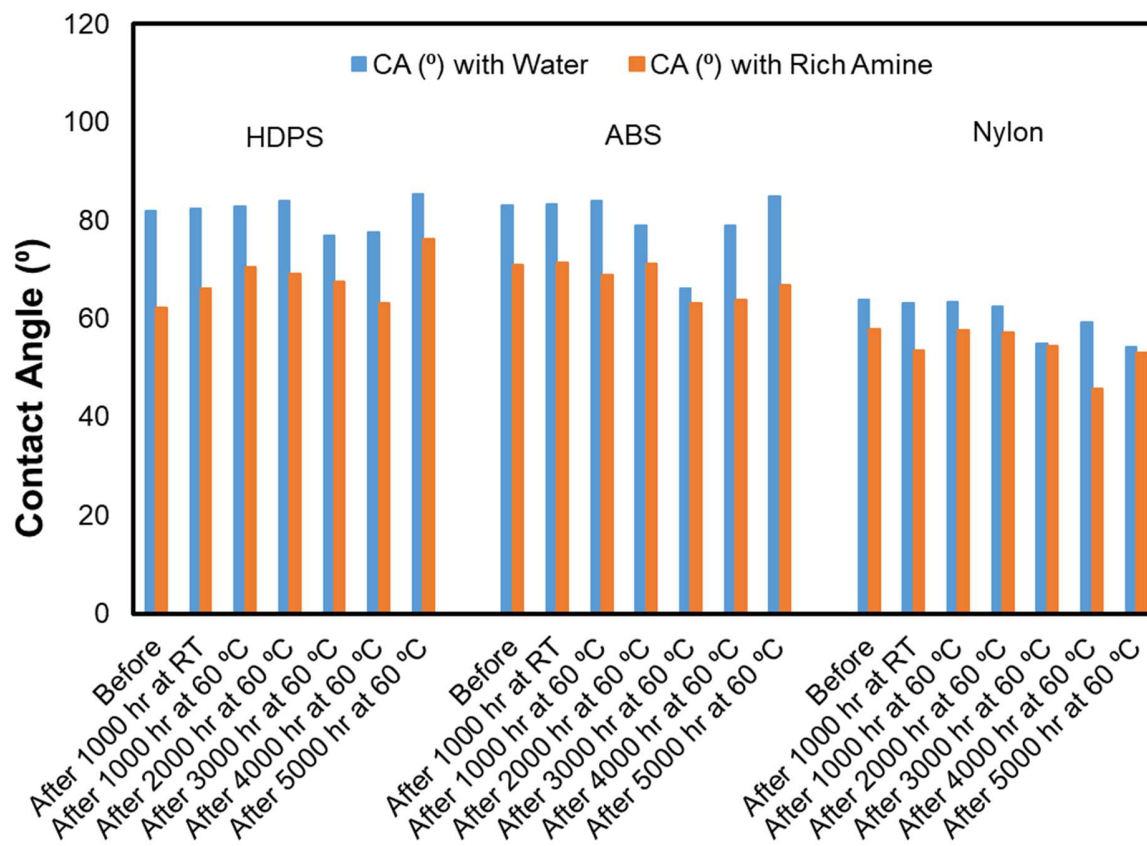
177 Information (See Supporting Information).

178

Figure 3. Contact angle (°) of polymer coupons after exposure to CO_2-loaded amine solvent.

180 Based on the values obtained of the contact angle of water on these polymers, these are generally

181 hydrophilic by having contact angles < 90° (Yuan and Lee, 2013). Nylon has a higher degree of

182 hydrophilicity, with both HDPS and ABS being closer to the transition point between

183 hydrophobic and hydrophilic at 90° contact angle. The contact angle of the amine solution on all

184 three polymer surfaces is lower when compared with water, likely due to the amine component.

185 In terms of the contact angle of the amine solution, generally all three of the polymers showed

186 minimal changes even after the 5000 hr exposure at 60 °C. The contact angle of the amine

187 solution on the HDPS polymer slightly increased, while for ABS, showed a slight increase.

188 Lastly, the Nylon surface appears to have slightly decreased. A decrease in contact angle after

189 amine exposure can be viewed positively as this translates to enhancement wetting of this

190 surface. Overall, the changes in contact angles were small and generally within the deviation of

191 the contact angle measurement method.

3.3. Contact angle and CO$_2$-loading

193 Next, the impact of changes to the CO$_2$-loading in a representative primary amine solution and

194 contact angle was evaluated. In addition to the polymer surfaces, the contact angle measurement

195 was done using a stainless-steel surface (**Figure 4**). As noted earlier, the contact angle of the

196 water is higher than the amine solution even on the stainless-steel surface. More interestingly,

197 there is a trend of increasing contact angle with higher CO$_2$-loading, observed on all the surfaces,

198 including the stainless steel. This shows that as the carbon loading of the solvent increases, the

199 wettability of the solution on packing material surfaces will decrease. This translates to less

200 wetting at the bottom of the absorber column where the reaction kinetics are already slowing

201 down. The less wetting will translate to a less active interfacial surface for mass transfer and

202 make the bottom packing section of the absorber making it less effective regardless of the

203 packing material composition. Nylon has the most similar contact angles to stainless steel

204 making this a good base material for further testing. While the contact angles of all these

205 polymers are higher than stainless steel, solvent additives can be used to drop the surface tension

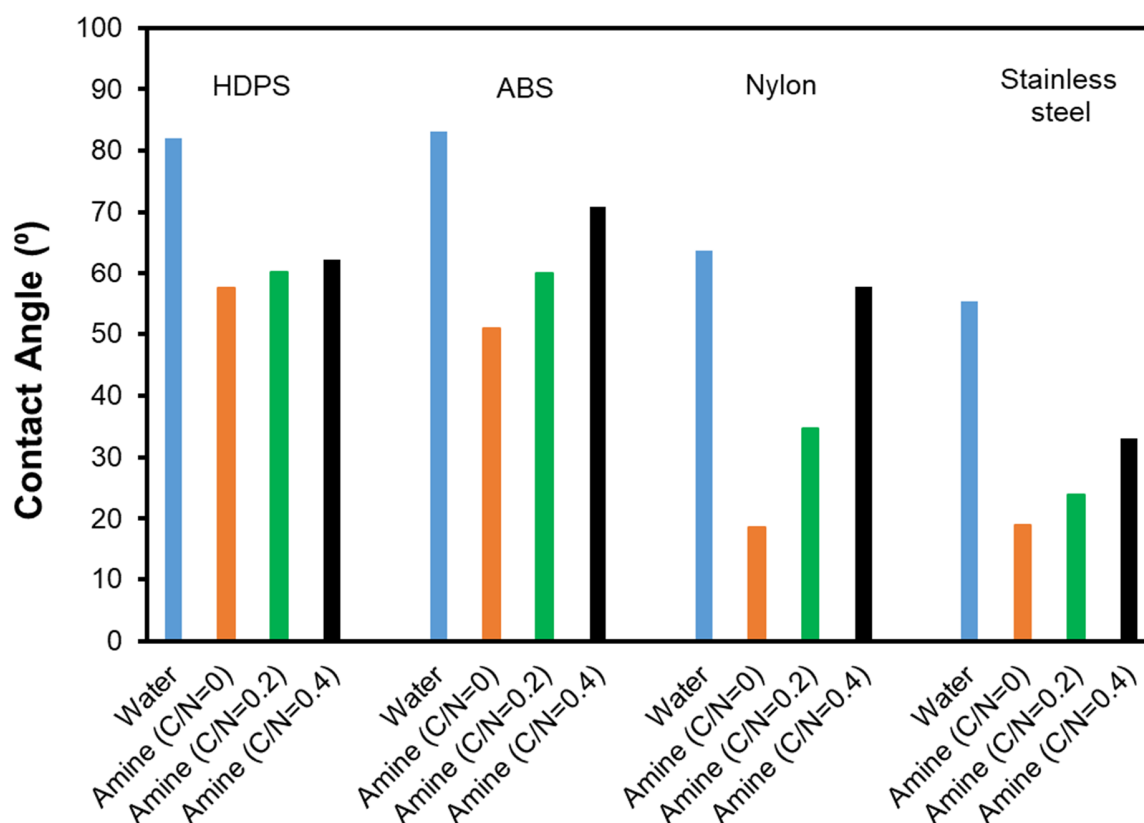206 and decrease the contact angle of the solvent at the bottom of the column.

Figure 4. Contact angle (°) of polymer and stainless surfaces after exposure to CO_2-loaded amine solvent.

The trend of an increase in contact angle with higher CO_2-loading was also observed in a set of seven commonly used primary, secondary, and tertiary amine solutions (**Figure 5**). The amines used in these studies are 5M Monoethanolamine (MEA), 5M 2-Amino-1 Propanol (2A1P), 5M N-Methylethanolamine (NMEA), 5M 2-(Ethylamino)ethanol (2EAE), 5M Dimethylethanolamine (DMEA), 5M Diethanolamine (DEA) and 5M N-Methyldiethanolamine (MDEA). The contact angles were measured on the ABS surface for comparison for all these aqueous amines. Every amine examined showed at least some degree of increase in its contact angle as the CO_2-loading also increased. Higher carbon loading in the solution results in high

218   viscosity and high surface tension(Widger et al., 2017). This shows that with commonly used

219   amines solvents, a decrease in wetting can be expected as they become CO_2-loaded and move

220   down the absorber column. Based on this data any method to improve solvent wetting can likely

221   be applied to a wider set of amine solvents including the inclusion of additives, such as

222   surfactants, that can increase the wettability of these solvents by lowing the solution surface

223   tension(Bryant et al., 2016). A table for static contact angles with aqueous amine on ABS surface

224   at different carbon loadings is reported in the Supporting Information (See Supporting
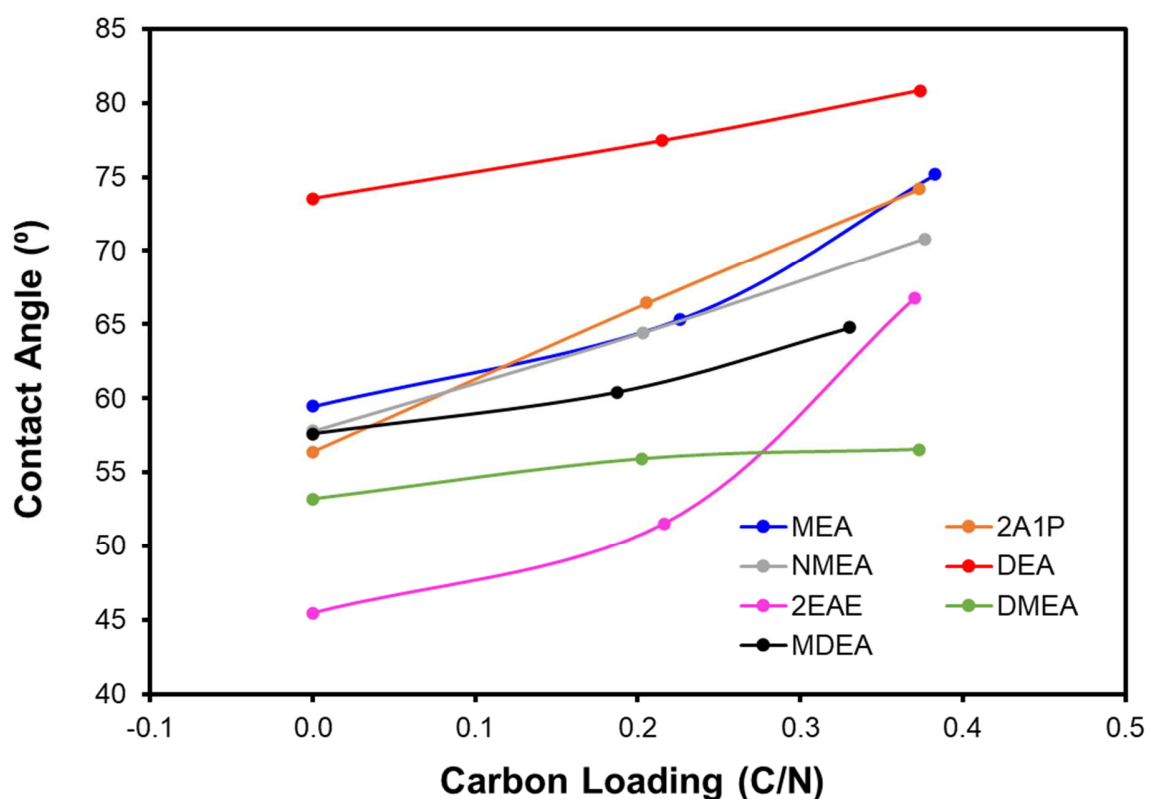
225   Information).

226

227   **Figure 5.** Contact angles of selected primary, secondary, and tertiary aqueous amine solutions at

228   unloaded (C/N=0), CO_2-lean (C/N~0.2) and CO_2-rich (C/N~0.4) loading on ABS surface.

4. Conclusions

Four polymers, commonly used for 3D printing were evaluated for physical and surface stability during long-term exposure to a CO_2-loaded amine solution at elevated temperatures typically observed in the absorber column. Three polymers, HDPS, ABS and, Nylon were found to be physically stable after 5000 hr of amine exposure at temperatures up to 60 °C. The wettabilities of the polymer surfaces were also stable after exposure to the CO_2-loaded amine solution. This study identifies several polymers that should be further tested to improve CO_2 capture performance inside the absorber column.

Competing financial interest

The authors declare no competing financial interest.

Acknowledgements

References

Boot-Handford, M.E., Abanades, J.C., Anthony, E.J., Blunt, M.J., Brandani, S., Mac Dowell, N., Fernández, J.R., Ferrari, M.-C., Gross, R., Hallett, J.P., Haszeldine, R.S., Heptonstall, P., Lyngfelt, A., Makuch, Z., Mangano, E., Porter, R.T.J., Pourkashanian, M., Rochelle, G.T., Shah, N., Yao, J.G., Fennell, P.S., 2014. Carbon capture and storage update. Energy & Environmental Science 7, 130-189.

Breidenich, C., Magraw, D., Rowley, A., Rubin, J.W., 1998. The Kyoto Protocol to the United Nations Framework Convention on Climate Change. American Journal of International Law 92, 315-331.

Bryant, J.J., Lippert, C., Qi, G., Liu, K., Mannel, D.S., Liu, K., 2016. Enhanced Carbon Capture through Incorporation of Surfactant Additives. Industrial & engineering chemistry research 55, 7456-7461.

Bui, M., Adjiman, C.S., Bardow, A., Anthony, E.J., Boston, A., Brown, S., Fennell, P.S., Fuss, S., Galindo, A., Hackett, L.A., Hallett, J.P., Herzog, H.J., Jackson, G., Kemper, J., Krevor, S., Maitland, G.C., Matuszewski, M., Metcalfe, I.S., Petit, C., Puxty, G., Reimer, J., Reiner, D.M., Rubin, E.S., Scott, S.A., Shah, N., Smit, B., Trusler, J.P.M., Webley, P., Wilcox, J., Mac Dowell, N., 2018. Carbon capture and storage (CCS): the way forward. Energy & Environmental Science 11, 1062-1176.

Floyd, W.C., Baker, S.E., Valdez, C.A., Stolaroff, J.K., Bearinger, J.P., Satcher, J.H., Aines, R.D., 2013. Evaluation of a Carbonic Anhydrase Mimic for Industrial Carbon Capture. Environmental Science & Technology 47, 10049-10055.

Frimpong, R.A., Nikolic, H., Pelgen, J., Ghorbanian, M., Figueroa, J.D., Liu, K., 2019. Evaluation of different solvent performance in a 0.7MWe pilot scale CO_2 capture unit. Chemical Engineering Research and Design 148, 11-20.

Inagaki, N., Kimura, H., 2009. Electroless copper plating on acrylonitrile butadiene styrene material surfaces without chromic acid etching and a palladium catalyst. Journal of applied polymer science 111, 1034-1044.

Koziol, L., Valdez, C.A., Baker, S.E., Lau, E.Y., Floyd, W.C., Wong, S.E., Satcher, J.H., Lightstone, F.C., Aines, R.D., 2012. Toward a Small Molecule, Biomimetic Carbonic Anhydrase Model: Theoretical and Experimental Investigations of a Panel of Zinc(II) Aza-Macrocyclic Catalysts. Inorganic Chemistry 51, 6803-6812.

Law, K.-Y., 2014. Definitions for Hydrophilicity, Hydrophobicity, and Superhydrophobicity: Getting the Basics Right. The journal of physical chemistry letters 5, 686-688.

Leclaire, J., Heldebrant, D.J., 2018. A call to (green) arms: A rallying cry for green chemistry and engineering for CO_2 capture, utilisation and storage. Green chemistry : an international journal and green chemistry resource : GC 20, 5058-5081.

Li, L., Voice, A.K., Li, H., Namjoshi, O., Nguyen, T., Du, Y., Rochelle, G.T., 2013. Amine blends using concentrated piperazine. Energy Procedia 37, 353-369.

Lin, P.-H., Wong, D.S.H., 2014. Carbon dioxide capture and regeneration with amine/alcohol/water blends. International Journal of Greenhouse Gas Control 26, 69-75.

Lippert, C.A., Liu, K., Sarma, M., Parkin, S.R., Remias, J.E., Brandewie, C.M., Odom, S.A., Liu, K., 2014. Improving carbon capture from power plant emissions with zinc- and cobalt-based catalysts. Catalysis science & technology 4, 3620-3625.

Liu, K., Widger, L.R., Fan, Z., Stolaroff, J., 2019. Method and apparatus for increasing mass transfer in aqueous gas adsorption processes, US20190176080 A1, U.S. Pat. Appl. Publ., USA.

Masson-Delmotte, V., P. Zhai, H.-O. Pörtner, D. Roberts, J. Skea, P.R. Shukla, A. Pirani, W. Moufouma-Okia, C. Péan, R. Pidcock, S. Connors, J.B.R. Matthews, Y. Chen, X. Zhou, M.I. Gomis, E. Lonnoy, T. Maycock, M. Tignor, and T. Waterfield 2018. Summary for Policymakers. In: Global Warming of 1.5°C. An IPCC Special Report on the impacts of global warming of 1.5°C above pre-industrial levels and related global greenhouse gas emission pathways, in the context of strengthening the global response to the threat of climate change, sustainable development, and efforts to eradicate poverty. 32.

Matin, N.S., Thompson, J., Onneweer, F.M., Liu, K., 2016. Thermal Degradation Rate of 2-Amino-2-methyl-1-propanol to Cyclic 4,4-Dimethyl-1,3-oxazolidin-2-one: Experiments and Kinetics Modeling. Industrial & Engineering Chemistry Research 55, 9586-9593.

Rochelle, G.T., 2009. Amine Scrubbing for CO_2 Capture. Science (AAAS) 325, 1652-1654.

Rodríguez-Vidal, E., Sanz, C., Etxarri, J., Bejarano, A., Lebour, Y., Malet, R., 2018. Modification of ABS wetting properties by ultrashort and short pulse lasers. Procedia CIRP 74, 568-572.

Rogelj, J., den Elzen, M., Höhne, N., Fransen, T., Fekete, H., Winkler, H., Schaeffer, R., Sha, F., Riahi, K., Meinshausen, M., 2016. Paris Agreement climate proposals need a boost to keep warming well below 2 °C. Nature 534, 631-639.

Shi, H., Naami, A., Idem, R., Tontiwachwuthikul, P., 2014. Catalytic and non catalytic solvent regeneration during absorption-based CO_2 capture with single and blended reactive amine solvents. International Journal of Greenhouse Gas Control 26, 39-50.

Stlaroff, J.K., 2017. High-efficiency, integrated reactors for sorbents, solvents, and membranes using additive manufacturing, 2017 NETL CO_2 Capture Technology Project Review Meeting.

Tsai, R.E., Schultheiss, P., Kettner, A., Lewis, J.C., Seibert, A.F., Eldridge, R.B., Rochelle, G.T., 2008. Influence of Surface Tension on Effective Packing Area. Industrial & Engineering Chemistry Research 47, 1253-1260.

306 Tsai, R.E., Seibert, A.F., Eldridge, R.B., Rochelle, G.T., 2011. A dimensionless model for predicting the
307 mass-transfer area of structured packing. AIChE Journal 57, 1173-1184.
308 Voice, A.K., Vevelstad, S.J., Chen, X., Nguyen, T., Rochelle, G.T., 2013. Aqueous 3-
309 (methylamino)propylamine for CO_2 capture. International Journal of Greenhouse Gas Control 15, 70-77.
310 Wang, M., Lawal, A., Stephenson, P., Sidders, J., Ramshaw, C., 2011. Post-combustion CO_2 capture with
311 chemical absorption: A state-of-the-art review. Chemical Engineering Research and Design 89, 1609-
312 1624.
313 Widger, L., Sarma, M., Bryant, J., Mannel, D., Thompson, J., Lippert, C., Liu, K., 2017. Enhancements in
314 mass transfer for carbon capture solvents part I: Homogeneous catalyst. International Journal of
315 Greenhouse Gas Control 63, 249-259.
316 Widger, L.R., Sarma, M., Kelsey, R.A., Risko, C., Lippert, C.A., Parkin, S.R., Liu, K., 2019. Enhancing
317 CO_2 absorption for post-combustion carbon capture via zinc-based biomimetic catalysts in industrially
318 relevant amine solutions. International Journal of Greenhouse Gas Control 85, 156-165.
319 Yang, H., Xu, Z., Fan, M., Gupta, R., Slimane, R.B., Bland, A.E., Wright, I., 2008. Progress in carbon
320 dioxide separation and capture: A review. Journal of Environmental Sciences 20, 14-27.
321 Yuan, Y., Lee, T.R., 2013. Contact Angle and Wetting Properties, in: Bracco, G., Holst, B. (Eds.),
322 Surface Science Techniques. Springer Berlin Heidelberg, Berlin, Heidelberg, pp. 3-34.
323 Zheng, R.F., Barpaga, D., Mathias, P.M., Malhotra, D., Koech, P.K., Jiang, Y., Bhakta, M., Lail, M., V.
324 Rayer, A., Whyatt, G.A., Freeman, C.J., Zwoster, A.J., Weitz, K.K., Heldebrant, D.J., 2020. A single-
325 component water-lean post-combustion CO_2 capture solvent with exceptionally low operational heat and
326 total costs of capture – comprehensive experimental and theoretical evaluation. Energy & Environmental
327 Science 13, 4106-4113.

328